

## Time- and space-resolved light emission and spectroscopic research of the flashover plasma

J. Z. Gleizer,<sup>1</sup> Ya. E. Krasik,<sup>1</sup> and J. Leopold<sup>2</sup>

<sup>1</sup>Physics Department, Technion, Haifa 32000, Israel

<sup>2</sup>Department of Applied Physics, Rafael Laboratories, Box 2250, Haifa 31021, Israel

(Received 5 January 2015; accepted 7 February 2015; published online 19 February 2015)

The results of an experimental study of the evolution of surface flashover across the surface of an insulator in vacuum subject to a high-voltage pulse and the parameters of the flashover plasma are reported. For the system studied, flashover is always initiated at the cathode triple junctions. Using time-resolved framing photography of the plasma light emission the velocity of the light emission propagation along the surface of the insulator was found to be  $\sim 2.5 \cdot 10^8$  cm/s. Spectroscopic measurements show that the flashover is characterized by a plasma density of  $2\text{--}4 \times 10^{14}$  cm<sup>-3</sup> and neutral and electron temperatures of 2–4 eV and 1–3 eV, respectively, corresponding to a plasma conductivity of  $\sim 0.2$   $\Omega^{-1}$  cm<sup>-1</sup> and a discharge current density of up to  $\sim 10$  kA/cm<sup>2</sup>. © 2015 AIP Publishing LLC. [<http://dx.doi.org/10.1063/1.4913213>]

### I. INTRODUCTION

Surface breakdown over insulators in vacuum is one of the most common limiting and costly factors in the operation of pulsed power systems. The study of this subject is very old,<sup>1</sup> yet the mechanism of the breakdown process and ways to avoid its occurrence are still not fully understood. Since in practice, vacuum is limited to a finite background pressure, conductor surfaces are never perfectly smooth because of micro-protrusions and insulator surfaces often contain microscopic voids filled with gas remnants—it is difficult to exactly define the system and the generality of experimental conclusions should be carefully considered. Because it is assumed that the difference in dielectric constants enhances the electric field near a triple junction, it is commonly accepted that triple junctions of the conductor-insulator-vacuum are the initiating regions of a surface flashover and that high surface voltage gradients enhance breakdown. To reduce the voltage gradient along the dielectric surface very large insulators were often used<sup>2</sup> and attempts to shield triple junctions<sup>3</sup> were also made to avoid flashover and breakdown. Flashover is defined as plasma discharge across the surface which shorts the voltage and allows current to flow between a cathode and an anode separated by the insulator in vacuum. If flashover processes persist, breakdown accompanied by insulator damage may occur thus permanently damaging the insulation properties. A conditioning process is usually used to determine the flashover field of a vacuum insulator.<sup>4</sup>

It is also accepted that the evolution of flashover is governed by charged primary particles which impact the surface of the insulator causing the development of a secondary electron avalanche. In Ref. 5, a rather good review of analytical and numerical investigations of electric field enhancement at a triple junction for different geometries of the interface insulator is presented. In this paper, the authors developed approximate analytical expressions for electric field enhancement at triple junctions and calculated trajectories of single seed electrons at the cathode triple junction (CTJ) for different

insulator inclination angles with respect to the cathode electrode. The results of these simulations showed good agreement with experiment. Namely, it was shown that when the angle between the insulator surface and cathode is  $< 90^\circ$ , the electric field distribution leads to acceleration of the seeded electron towards the dielectric surface. This electron acquires the energy sufficient for secondary electron emission and, respectively, for avalanche generation. In Ref. 6, it was suggested that voltage holdoff will considerably improve if primary electrons are deflected away from impacting while at the same time secondary electrons are accelerated away from the insulator surface so these electrons cannot restrike. Such a scheme is made possible by appropriate design of the orientation of the electric and magnetic fields near the insulator surface. This conjecture was confirmed in experiments where the orientation and magnitude of the electric fields were manipulated and the flashover fields along the surface of such insulator samples were measured.<sup>4</sup> Moreover, it was deduced that when an axially symmetric insulator block separates the parallel surfaces of a cathode and an anode, flashover was always initiated near the CTJ.<sup>4</sup>

The electric field at a perfect triple junction of perfect insulator, conductor surfaces, and absolute vacuum is known analytically.<sup>7</sup> In particular, when at the anode triple junction (ATJ), the inclination angle of the insulator surface is  $\pi/2 < \beta_A \leq 3\pi/4$ , relative to a flat conducting surface,  $\alpha_A = \pi$ , the electric field approaches infinity (see Fig. 1). This seemed to support the assumption that the flashover for this case is initiated at the ATJ.<sup>8</sup> However, in Ref. 4, it was shown that whether the electric field at the ATJ is infinite, zero or a value in between, it has no effect on the flashover field.

The evolution of light emission from the surface flashover of vacuum insulators was studied in Refs. 9–13. In an early study<sup>9</sup> using fast framing imaging, it was shown that the light emission of the discharge channel initiated at the cathode triple junctions propagates along forsterite ceramic at a speed reaching  $2.7 \times 10^7$  cm/s for an electric field of  $\sim 140$  kV/cm and background pressure of  $\sim 2$  mPa. A similar

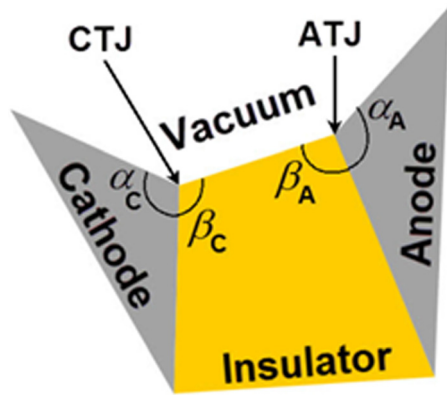


FIG. 1. The definition of the orientation angles<sup>6</sup> between the various surfaces in a z-directionally symmetric plane for a situation where an insulator separates a cathode from an anode in vacuum.

velocity ( $\sim 1.5 \times 10^7$  cm/s) of light front propagation was obtained in Ref. 10 where a streak camera was used to study time-resolved evolution of the flashover along the surface of n-type silicon with an applied average electric field of  $\sim 30$  kV/cm. A larger velocity, up to  $5 \times 10^8$  cm/s of light emission front propagation initiated at the CTJ was observed in experiments with polymethyl methacrylate subject to a 100 kV/cm pulse with a 30 ns rise time.<sup>11</sup> In these experiments, multi-framing fast intensified camera was employed. In Ref. 12, fast framing imaging was applied to estimate the velocity of the plasma front propagation along the surface of polyethylene or polycarbonate insulator inclined to  $\beta_C = 45^\circ$ . In these experiments, the flashover was initiated by the electron emission from the plasma generated from a velvet “dot” placed at different locations on the conducting electrodes. It was shown that the flashover could be initiated not only near the CTJ but near the ATJ as well. The velocity of the light emitting plasma front propagation was found to be  $\sim 2.4 \times 10^6$  cm/s at the average electric field of  $\sim 100$  kV/cm, which is  $\sim 10$  times smaller than that obtained in experiments.<sup>9–11</sup> Recently, results of experiments<sup>13</sup> were presented where the evolution of the flashover between electrodes placed on an alumina surface in vacuum was recorded by a fast intensified framing camera. In these experiments, the curvature of the conducting surfaces facing each other was changed. All cases studied in Ref. 13 correspond to  $\beta_C = \beta_A = \pi$  (see Fig. 1) for both the CTJ and the ATJ along all junction lines connecting between the conductors and the insulator surface. At the same time  $0 \leq \alpha_A, \alpha_C \leq \pi/2$ ,  $0.5 \leq \nu \leq 0.55$ ,<sup>6</sup> that is, the electric field approaches infinity for both the CTJ and ATJ and the curvature parameter studied in Ref. 13 affects only the distance between these junction lines. When the curvature of the anode surface was such that it formed a 0.1 mm sharp tip, anode initiated flashover was observed, otherwise all other cases showed that flashover was initiated at the CTJ.

Spectroscopic measurements of the flashover plasma were reported too.<sup>14,15</sup> In Ref. 14, an Alumina insulator in vacuum was tested and  $N_2$  and AlO molecular bands together with H and Al I, Al II, and Al III spectral lines were recorded. These data indicate that desorbed gases and material defects contributed to the flashover process. In Ref. 15,

both time-resolved imaging of the plasma light emission and visible spectroscopy were employed to study the flashover process across alumina placed between ball shaped electrodes in vacuum. It was shown that the spectrum of the plasma is characterized by the existence of hydrogen and carbon ions prior to complete shorting of the insulator by flashover plasma. However, the density and temperature of the flashover plasma were not studied so far.

In the present paper, experimental results on the evolution of flashover over the surface of a vacuum insulator subject to a high-voltage pulse and parameters of the flashover plasma are presented. In our experiments, we observe that flashover is always initiated from the CTJ.

## II. EXPERIMENTAL SETUP

The experimental setup described in Ref. 4 (see Fig. 2) was used to study the parameters of the plasma generated as a result of flashover over the surface of an insulator in vacuum. A positive polarity high-voltage pulse with amplitudes up to 300 kV and rise time of  $\sim 30$  ns generated by a Marx generator was applied over the dielectric sample placed between 130 mm diameter highly polished stainless steel anode and cathode electrodes. Polypropylene or Plexiglas (Polymethyl-methacrylate) 50 mm diameter, 15–20 mm high cylindrical insulator samples were used. In order to facilitate the initiation of the surface flashover from a fixed location a thin (50  $\mu$ m) and 1.5–3 mm high copper triangular foil (igniter) was attached to the insulator surface at either the cathode or anode end.

A turbo-molecular pump kept the background pressure in the experimental chamber  $\leq 6.5$  mPa. The voltage and current waveforms were measured by a resistive voltage divider and a self-integrated Rogowski coil, respectively. The light emission from the surface flashover plasma was observed using a 4QuikE intensified camera synchronized relative to the beginning of the high-voltage pulse. Waveforms of the voltage, current, and the camera’s synchronized pulse for a flashover occurrence are shown in Fig. 3 for the case when the igniter was placed at the cathode end. One can see that the flashover associated with a fast decrease in the voltage, starts when the voltage

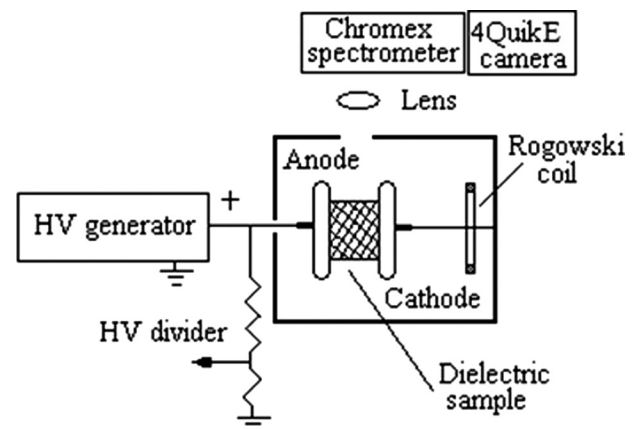


FIG. 2. Experimental setup.

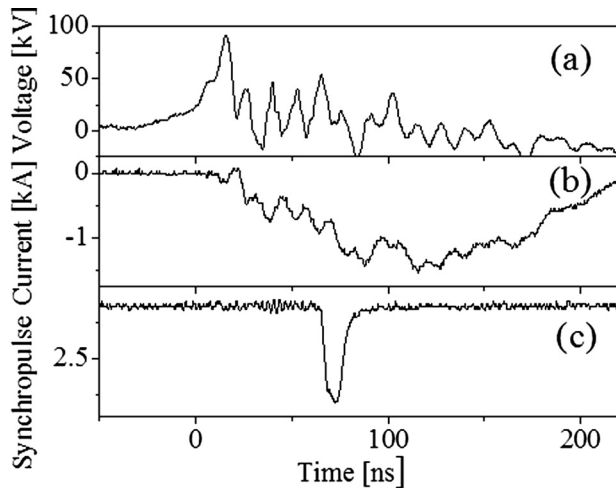


FIG. 3. Typical waveforms of voltage (a), current (b), and fast camera synchronized pulse (c) for the case of 15 mm polypropylene sample.

amplitude reaches  $\sim 90$  kV, corresponding to the average electric field of  $\sim 60$  kV/cm. Let us note here that in the case of the absence of the igniter, the flashover for cylindrical form insulator of 15 mm height was obtained at  $\sim 160$  kV/cm.<sup>4</sup> A decrease in  $\sim 2.7$  times in the threshold of the breakdown field is evidently due to electric field enhancement at the tip of the igniter.

Spectroscopic measurements of the plasma parameters (density and temperature) were carried out by analyzing the hydrogen atom  $H_\alpha$  and  $H_\beta$  spectral line intensities using 250 mm Chromex imaging spectrometer. The spectral resolution of the spectrometer ( $0.4 \text{ \AA}/\text{pix}$  and  $2.4 \text{ \AA}/\text{pix}$  for 1800 g/mm and 150 g/mm gratings, respectively) and the instrumental full width at half maximum (FWHM) in the spectral range of 4000–6600  $\text{\AA}$  were determined by Oriol spectral lamps. The FWHM of the  $H_\alpha$  and  $H_\beta$  spectral lines and relative intensities of these lines were measured using 1800 g/mm and 150 g/mm gratings, respectively. The latter allows to obtain these spectral lines in one shot of the generator. The spectral line intensity was recorded by the 4QuikE camera placed at the output of the spectrometer. The frame duration of the camera was  $\geq 100$  ns; at smaller exposure time, the flux of light was insufficient to obtain reliable spectral line profile. The width of the input slit of the spectrometer was  $100 \mu\text{m}$  which allowed us to obtain the plasma parameters at three different distances from the cathode igniter, namely, at  $1 \pm 0.2$  mm,  $7 \pm 0.2$  mm, and  $11 \pm 0.2$  mm. For each position and for each spectral line at least 3 generator shots were carried out.

### III. EXPERIMENTAL RESULTS

#### A. Light emission of the flashover plasma

Light emission images of flashover plasma obtained across a 15 mm Polypropylene sample surface with an igniter placed at the cathode end at different time delays  $t_d$  with respect to the beginning of the fast decrease in the applied voltage are shown in Fig. 4. As expected, one can see that flashover process along dielectric surface is initiated at the location of the igniter tip (see Fig. 4(a)) with plasma light emission (see Fig. 4(a)) becoming visible at  $t_d \geq 4$  ns. The width of the plasma channel at initial stage of surface discharge (Fig. 4(b),  $t_d \approx 8$  ns) was  $\leq 0.5$  mm and it increases up to  $\sim 1$  mm during the discharge (Figs. 4(c) and 4(d),  $t_d \approx 26$ – $34$  ns). Also, one can see that the brighter light emission during the initial stage of discharge occurs at the cathode side (Fig. 4(b),  $t_d \approx 8$  ns). Later, the light emission from the plasma channel became almost uniform (Fig. 4(c),  $t_d \approx 26$  ns) and at  $t_d > 35$  ns the light emission becomes more intense at locations close to the anode and cathode than from the middle of the insulator (Fig. 4(d),  $t_d \approx 34$  ns). The same evolution of the light emission of the flashover plasma was obtained for 20 mm in height and 80 mm in diameter polypropylene sample. The velocity of the plasma visible light emission propagation along the insulator surface can be estimated as  $3 \pm 1 \times 10^8$  cm/s.

Similar images (see Fig. 5) of the light emission of the flashover plasma were obtained for 15 mm high Plexiglas samples. The only differences were that in this case the observed light emission was significantly more intense than for polypropylene (for the same magnification on the 4QuikE camera). Also, for Plexiglas, the discharge channel splits as it approaches the anode.

The images seen in Figs. 4 and 5 are not unique and for all cases considered with an igniter attached at the cathode end, flashover was initiated at the tip of the cathode igniter. The insulator samples were cylindrical and the electric field along all junction lines equals the average electric field at the start of the flashover ( $\sim 60$  kV/cm) apart from along the igniter where it is infinite.

Finally, when the igniter triangle was attached to the anode end no flashover developed from its tip, even when its length was increased to 5 mm. When flashover developed with an anode igniter it was initiated randomly along the triple junction vacuum-insulator-cathode intersection line. For this case the flashover field was higher,  $\sim 150$  kV/cm, similar to values obtained in Ref. 4. The fact that the electric field at

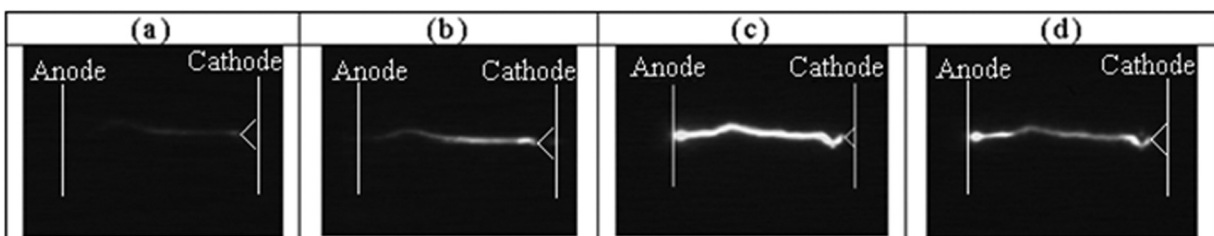


FIG. 4. Images of flashover plasma along a 15 mm high, 50 mm diameter Polypropylene sample. (a)  $t_d \approx 4$  ns, MCP voltage: 860 V; (b)  $t_d \approx 8$  ns, MCP voltage: 860 V; (c)  $t_d \approx 26$  ns, MCP voltage: 750 V; (d)  $t_d \approx 34$  ns, MCP voltage: 750 V. Frame duration is 5 ns.

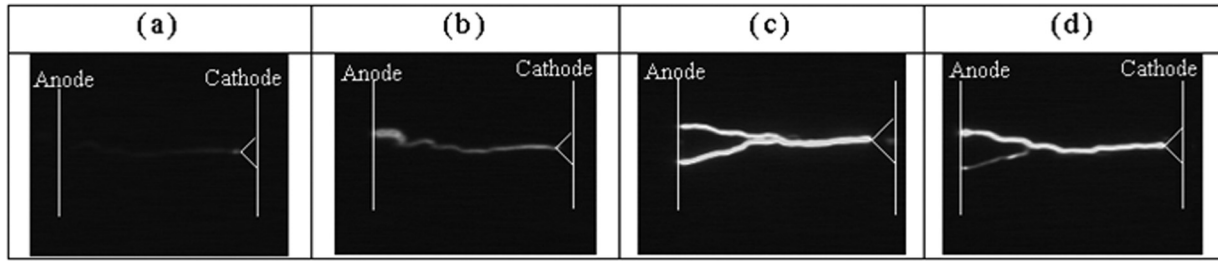


FIG. 5. Images of flashover plasma along a 15 mm high, 50 mm diameter Plexiglas sample. (a)  $t_d \approx 4$  ns, MCP voltage of 600 V; (b)  $t_d \approx 9$  ns, MCP voltage: 650 V; (c)  $t_d \approx 11$  ns, MCP voltage: 620 V; (d)  $t_d \approx 18$  ns, MCP voltage: 600 V; Frame duration is 5 ns.

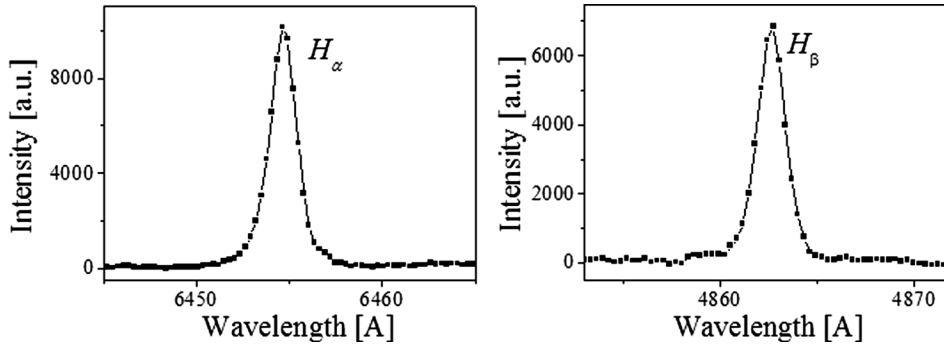


FIG. 6. Typical  $H_\alpha$  and  $H_\beta$  spectral lines obtained at  $t_d \approx 50$  ns with frame duration of 300 ns during the flashover of the polypropylene sample at 2 mm from the cathode.

the anode igniter triple junction is infinite did not affect the flashover process which is electron initiated.

## B. Spectroscopic measurements

To obtain the density and the temperature of the flashover plasma, hydrogen atom  $H_\alpha$  and  $H_\beta$  spectral lines were measured and analyzed (see Fig. 6). The width of the  $H_\alpha$  spectral line represents the Doppler broadening of this line  $\Delta\lambda_{H_\alpha}[\text{\AA}] = 0.515\sqrt{T_H[\text{eV}]}$ . The latter was used to obtain the hydrogen temperature near the cathode, at the center of the insulator sample and near the anode. Indeed,  $H_\alpha$  spectral line is significantly less sensitive to Stark broadening than  $H_\beta$  spectral line.<sup>16</sup> The measured FWHM  $\Delta\lambda_V$  of the  $H_\alpha$  spectral line intensity presents Voigt profile. The latter is a convolution of Lorentzian profile due to the Stark broadening  $\Delta\lambda_S$  and two Gaussian profiles due to instrumental  $\Delta\lambda_{instr}$  and Doppler  $\Delta\lambda_D$  broadenings. Convolution of these two Gaussian profiles also gives a Gaussian profile with  $\Delta\lambda_G^2 = \Delta\lambda_{instr}^2 + \Delta\lambda_D^2$ . Using the expression for the Voigt profile, one obtains the Doppler broadening of the spectral line as:  $\Delta\lambda_D \approx \sqrt{(\Delta\lambda_V - 0.5346\Delta\lambda_S)^2 - 0.2166\Delta\lambda_S^2 - \Delta\lambda_{instr}^2}$ . In the spectroscopic setup used in this experiment the instrumental broadening of the spectral line was  $\Delta\lambda_{instr} \approx 1.1 \text{\AA}$  and the Stark broadening for the  $H_\alpha$  line  $\Delta\lambda_{SH_\alpha} \leq 0.3 \text{\AA}$  (Ref. 15) for the plasma density  $n_e \leq 5 \cdot 10^{14} \text{cm}^{-3}$ . The temperature of hydrogen atoms at different distances from the cathode are given in Table I. One can see that the

TABLE I. Hydrogen atoms temperature.

Distance from the cathode igniter (mm)	1 ± 0.2	7 ± 0.2	11 ± 0.2
Temperature (eV)	1.9 ± 0.6	2.4 ± 0.5	3.4 ± 0.4

temperature is increasing towards the anode which can be related to the spreading of the discharge plasma channel.

The FWHM of the Stark broadening,  $\Delta\lambda_{SH_\beta}$ , of the  $H_\beta$  spectral line due to micro-electric fields of the plasma charged particles was used to calculate plasma electron density using:<sup>16,17</sup>  $n_e(\text{cm}^{-3}) = C(n_e, T_e)\Delta\lambda_{SH_\beta}^{3/2}[\text{\AA}]$ , where  $C(n_e, T_e)$  is the coefficient which is only weakly depends on the electron density and temperature and can be assumed to be  $3.7 \times 10^{14} (\text{\AA}^{-3/2} \text{cm}^{-3})$  for plasma density in the range  $10^{14} \text{cm}^{-3}$  (the temperature in the range of 1–4 eV). The value of  $\Delta\lambda_{SH_\beta}$  was determined using the FWHM of the measured Voigt profile of the  $H_\beta$  spectral line and known values of the instrumental  $\Delta\lambda_{instr}$  and Doppler  $\Delta\lambda_{DH_\beta}[\text{\AA}] = 0.38\sqrt{T_H[\text{eV}]}$  broadenings. The values of the plasma density at different distances from the cathode are presented in Table II. One can see that the density of the discharge plasma channel decreases towards the anode which agrees with suggestion of the channel spreading.

Finally, the plasma electron temperature  $T_e$  is defined using the ratio of the intensities of the  $H_\alpha$  and  $H_\beta$  spectral lines obtained in one generator shot and assuming Boltzmann population of the excited energy levels

$$T_e = \frac{E_2 - E_1}{k_B} \left[ \ln \left( \frac{I_\alpha \lambda_\alpha g_2 A_2 k_2 P C k_2 \text{grating}}{I_\beta \lambda_\beta g_1 A_1 k_1 P C k_1 \text{grating}} \right) \right]^{-1},$$

where  $E_1$  and  $E_2$  are the upper energy levels of the  $H_\alpha$  and  $H_\beta$  transitions, respectively,  $I_\alpha$  and  $I_\beta$  are the  $H_\alpha$  and  $H_\beta$

TABLE II. Plasma electron density at different distances from the cathode.

Distance from the cathode igniter (mm)	1 ± 0.2	7 ± 0.2	11 ± 0.2
Electron density ( $\text{cm}^{-3}$ ) $\times 10^{14}$	3.2 ± 1.4	3.6 ± 0.4	2.8 ± 0.3

TABLE III. Plasma electron temperature.

Distance from the cathode (mm)	$1 \pm 0.2$	$7 \pm 0.2$	$11 \pm 0.2$
Temperature (eV)	$2.8 \pm 0.1$	$1.5 \pm 0.1$	$1 \pm 0.1$

relative line intensities,  $\lambda_\alpha$  and  $\lambda_\beta$  are the  $H_\alpha$  and  $H_\beta$  wavelengths,  $g_1, A_1$  and  $g_2, A_2$  are the statistical weights and Einstein coefficients of the  $H_\alpha$  and  $H_\beta$  upper levels, respectively,  $k_{1PC}$ ,  $k_{1grating}$  and  $k_{2PC}$ ,  $k_{2grating}$  are the quantum efficiency of the 4QuikE camera photo-cathode and grating at  $\lambda_\alpha$  and  $\lambda_\beta$ , respectively. The values of the plasma electron temperatures at different distances from the cathode are shown in Table III. One can see that the plasma electron temperature decreases towards the anode in qualitative agreement with the obtained decrease in the  $H_\beta$  spectral line intensity towards the anode.

#### IV. SUMMARY

We carried out a space- and time-resolved study of the light emission from the surface discharge plasma during vacuum insulator surface flashover. We show that the discharge is initiated only from the cathode end. The velocity of the light emission propagation which can be associated with the avalanche process along the surface of the insulator reaches  $\sim 2.5 \cdot 10^8$  cm/s. One can reasonable assume that this avalanche process is initiated at CTJ by electrons emitted from the cathode at that location. The assumption qualitative agrees with the results of simulations<sup>5,6</sup> of trajectories of electron emitted at CTJ and causing secondary electron emission from the insulator. The flashover plasma parameters determined by spectroscopic measurements determine that the plasma density was in the range of  $2-4 \times 10^{14}$  cm<sup>-3</sup> and neutral and electron temperatures 2–4 eV and 1–3 eV, respectively. With these plasma parameters, one can estimate the plasma conductivity to be  $\sim 0.2 \Omega^{-1}$  cm<sup>-1</sup> able to conduct a discharge current of density of up to  $\sim 10$  kA/cm<sup>2</sup>. Experiments with a 215 nm laser beam focused on the conductor surface in the vicinity of either the CTJ or ATJ are being planned at present. The energy of the photons is sufficient for photo-emission of electrons, thus the initiation of

the flashover process will be tested for different geometries of the insulator without a physical igniter.

#### ACKNOWLEDGMENTS

This work was supported by an RSF (Rafael Science Fund) grant. This fund was established to enhance scientific research collaboration between industry and academic institutions.

- <sup>1</sup>H. C. Miller, *IEEE Trans. Electr. Insul.* **24**, 765 (1989).
- <sup>2</sup>I. Smith, *IEEE Trans. Plasma Sci.* **34**, 1585 (2006).
- <sup>3</sup>S. Humphries, *Principles of Charged Particle Acceleration* (Wiley, New York, 1989).
- <sup>4</sup>J. Z. Gleizer, Ya. E. Krasik, U. Dai, and J. G. Leopold, *Trans. Dielectr. Electr. Insul.* **21**, 2394 (2014).
- <sup>5</sup>N. M. Jordan, Y. Y. Lau, David M. French, R. M. Gilgenbach, and P. Pengvanich, *J. Appl. Phys.* **102**, 033301 (2007).
- <sup>6</sup>J. G. Leopold, C. Leibovitz, I. Navon, and M. Markovits, *Phys. Rev. ST Accel. Beams* **10**, 060401 (2007).
- <sup>7</sup>M. S. Chung, B.-G. Yoon, P. H. Cutler, and N. M. Miskovsky, *J. Vac. Sci. Technol. B* **22**, 1240 (2004).
- <sup>8</sup>W. A. Stygar, J. A. Lott, T. C. Wagoner, V. Anaya, H. C. Harjes, H. C. Ives, Z. R. Wallace, G. R. Mowrer, R. W. Shoup, J. P. Corley, R. A. Anderson, G. E. Vogtlin, M. E. Savage, J. M. Elizondo, B. S. Stoltzfus, D. M. Andercyk, D. L. Fehl, T. F. Jaramillo, D. L. Johnson, D. H. McDaniel, D. A. Muirhead, J. M. Radman, J. J. Ramirez, L. E. Ramirez, R. B. Spielman, K. W. Struve, D. E. Walsh, E. D. Walsh, and M. D. Walsh, *Phys. Rev. ST Accel. Beams* **8**, 050401 (2005), and references therein.
- <sup>9</sup>S. P. Bugaev, A. M. Iskoldskii, and G. A. Mesyats, *Sov. Phys. – Techn. Phys.* **12**, 1358 (1968).
- <sup>10</sup>F. E. Peterkin, T. Ridolfi, L. L. Buresh, B. J. Hankla, D. K. Scott, P. F. Williams, W. C. Nunnally, and B. L. Thomas, *IEEE Trans. Electr. Dev.* **37**, 2459 (1990).
- <sup>11</sup>J. Tang, A. Qiu, L. Yang, W. Jia, H. Wang, and J. Li, *IEEE Trans. Plasma Sci.* **38**, 53 (2010).
- <sup>12</sup>J. B. Javedani, D. A. Goertz, T. L. Houck, E. J. Lauer, R. D. Speer, L. K. Tully, G. E. Vogtlin, and A. D. White, Report UCRL-TR-228713, Lawrence Livermore National Laboratory (2007).
- <sup>13</sup>G.-Q. Su, Y. Lang, J.-Y. Zhan, B.-P. Song, G.-J. Zhang, F. Li, and M. Wang, *IEEE Trans. Plasma Sci.* **42**, 2576 (2014).
- <sup>14</sup>C. R. Li, R. Sundararaman, and T. S. Sudarshan, *IEEE Trans. Plasma Sci.* **21**, 598–604 (1993).
- <sup>15</sup>A. A. Neuber, M. Butcher, H. Krompholz, L. L. Hatfield, and M. Kristiansen, *IEEE Trans. Plasma Sci.* **28**, 1593 (2000).
- <sup>16</sup>H. R. Griem, *Plasma Spectroscopy* (McGraw-Hill, New York, 1964).
- <sup>17</sup>M. A. Gigosos and V. Cardenoso, *J. Phys. B: At. Mol. Opt. Phys.* **29**, 4795 (1996).